Heteroaggregation of CeO_2 nanoparticles in presence of alginate and iron (III) oxide

Oriekhova, Olena; Stoll, Serge

How to cite

ORIEKHOVA, Olena, STOLL, Serge. Heteroaggregation of CeO_2 nanoparticles in presence of alginate and iron (III) oxide. In: Science of the Total Environment, 2019, vol. 648, p. 1171–1178. doi: 10.1016/j.scitotenv.2018.08.176

This publication URL: https://archive-ouverte.unige.ch/unige:107265
Publication DOI: 10.1016/j.scitotenv.2018.08.176

Heteroaggregation of CeO_2 nanoparticles in presence of alginate and iron (III) oxide

Olena Oriekhova*, Serge Stoll

Group of Environmental Physical Chemistry, Department F.-A. Forel for Environmental and Aquatic Sciences, Institute of Environmental Science, University of Geneva
Uni Carl Vogt 66, boulevard Carl-Vogt, CH-1211 Geneva 4, Switzerland;

* Corresponding author:
Olena Oriekhova (ORCID https://orcid.org/0000-0001-5885-4605)
Olena.Oriekhova@unige.ch
Tel: +41 22 379 0332.

Serge Stoll (ORCID https://orcid.org/0000-0003-3158-4208)
Serge.Stoll@unige.ch
Tel: +41 22 379 0333; fax: +41 22 379 0302

Abstract

When manufactured nanoparticles are released to natural waters, heteroaggregation between nanoparticles and water compounds is expected to occur and play a key role in nanoparticle fate, transport and transformation. In this work, the heteroaggregation between CeO_2 nanoparticles and Fe_2O_3 inorganic colloids, which represent the main inorganic fraction from Lake Geneva water, is studied. The heteroaggregation processes between CeO_2, Fe_2O_3 and alginate in multiple water samples are investigated using zeta potential and z-average diameter measurements. The kinetics of heteroaggregation of individual components as well as mixtures of CeO_2 nanoparticles and Fe_2O_3 colloids and alginate are studied using time resolved dynamic light scattering. The global attachment efficiency (α_{global}) is calculated using data from kinetic experiments. α_{global} for pristine CeO_2 nanoparticles varied from 0.5 to 0.7 in lake and synthetic waters and is found around 1 for pristine Fe_2O_3 and mixture CeO_2 and Fe_2O_3. Our findings demonstrate that heteroaggregation is highly dependent on environmental conditions and resulting electrostatic scenarios. No heteroaggregation at pH 8 between CeO_2, Fe_2O_3 and alginate is observed in ultrapure water, because of electrostatic repulsions between negatively charged compounds. In synthetic and lake waters, the situation is opposite. Indeed, specific adsorption of divalent cations and presence of salt are found to promote heteroaggregation via cation bridging and screening effects. The kinetic experiments indicate that aggregation rate of pristine Fe_2O_3 is higher (89 nm/min in lake water) compared to pristine CeO_2 nanoparticles (50 nm/min) and on the same level as mixture of CeO_2 and Fe_2O_3 (96 nm/min). Low alginate concentration, 0.25 mg/L, has no effect on heteroaggregation in mixture of CeO_2 and Fe_2O_3 in lake and synthetic waters. On the other hand, in natural water, the presence of higher alginate concentration, 2 mg/L, is found to reduce the heteroaggregation rate.

Keywords: CeO_2 nanoparticles, Fe_2O_3, alginate, heteroaggregation, lake water, cation adsorption

1. Introduction

The progress in nanotechnology has resulted to the wide commercial production and use of manufactured nanoparticles (NPs) increasing the concern about their accumulation and fate in environmental aquatic systems. Cerium dioxide (CeO_2) NPs are used in industry and everyday products and produced on the level from hundreds to thousand tons per year (Piccinno et al., 2012). The fate of CeO_2 NPs in natural aquatic systems depends on the MNP properties such as surface charge and size but also on the water chemistry including pH, ionic composition, presence of natural organic matter (NOM) and inorganic colloids.

Natural aquatic systems are highly heterogeneous systems which contain naturally occurring colloidal particles such as natural organic matter, biological colloids, inorganic colloids etc. Because of such heterogeneity, NPs released to natural waters are interacting with different water compounds resulting in aggregation or stabilisation. It is expected that concentration of NPs released to the water body is much lower than the concentration of naturally occurring colloids (Gondikas et al., 2014; Piccinno et al., 2012; Slomberg et al., 2016) resulting to heteroaggregation between NPs and natural colloids (Praetorius et al., 2014; Quik et al., 2012; Wang et al., 2015). Moreover, Quik et al. (2012) showed that the type of aggregation (homo- or heteroaggregation) was strongly dependent on the NP concentration. When the NP concentration released to river water is relatively high (10 and 100 mg/L), homoaggregation is dominant, contrary to the relatively low concentration (1 mg/L) for which heteroaggregation with natural colloids is the main mechanism for particle elimination (Quik et al., 2012).

In order to obtain input parameters (i.e. attachment efficiencies for heteroaggregation, α_{hetero}), which are independent on the NP concentration, to use in the environmental fate models, heteroaggregation of TiO_2 NPs with natural colloids (SiO_2

79 particles) was performed (Praetorius et al., 2014). Authors showed that α_{hetero} is
80 strongly dependent on solution ionic strength at pH 8 when NPs and natural colloids are
81 both negatively charged. It was also shown that NOM (humic acid) has a stabilising effect
82 on heteroaggregation. The experimental data were also used to obtain the global
83 aggregation rate (α_{global}) which represents overall the global behaviour of the
84 aggregating system, and, in particular, the formation of primary and secondary
85 aggregates (Praetorius et al., 2014).

86 Heteroaggregation of TiO_2 NPs with a smectite clay, which represents an
87 analogue of natural colloids, was evaluated to assess the main mechanisms controlling
88 the NP aggregation in natural environment (Labille et al., 2015). It was found that the
89 shape and dispersion state of colloids, the affinity and concentration ratio between
90 colloids and nanoparticles are the main parameters that affect heteroaggregation.
91 Moreover, authors showed that the presence of 1 mg/L humic acids reduce the
92 aggregation rate.

93 The importance of NOM on the NP aggregation and interaction between NPs and
94 ICs have been extensively studied separately. However, studies evaluating the impact of
95 NOM and ICs together on NP aggregation in natural environment are still limited. In our
96 work we concentrated mainly on the effect of two colloidal fractions, polysaccharides
97 and inorganic colloids. The choice of these two fractions is discussed below.

98 Alginate is a natural polysaccharide that represents up to 30% of NOM in lake
99 water (Buffle et al., 1998) and commonly used as a model polyelectrolyte to mimic
100 polysaccharides from natural waters (Chen et al., 2006). Alginate is a linear anionic
101 polymer with a negative linear charge and carboxylic acid groups on the chain backbone
102 (Pawar and Edgar, 2012). The stabilising effect of alginate coating on iron oxide
103 nanoparticles in biological media was shown by (Castelló et al. 2015). Alginate coated

iron oxide particles were found stable up to 9 days in biological fluids. Another study indicated that the adsorption of alginate on titanium dioxide NPs induces the partial fragmentation of already formed aggregates (Loosli et al., 2013).

Another component of natural water that is also expected to influence the fate and behaviour of NPs are inorganic colloids (ICs). The concentration of ICs in natural water is highly variable and can change from a few to hundreds mg/L (Eyrolle and Charmasson, 2004). The most common ICs are clays, aluminoscilicates and iron oxidyhydroxides (Eyrolle and Charmasson, 2004, 2001; Filella, 2007). For example, the concentration of suspended particulate matters in river Rhône varies from 3 to 40 mg/L and is mainly represented by the presence of clay minerals, calcite, quartz, muscovite and iron oxide (sampling of Rhône water near Arles) (Slomberg et al., 2016). Another study indicates the proportions of Fe and Al observed in the colloidal phase in the river Rhône freshwaters reached 42% and 35% respectively (Eyrolle and Charmasson, 2004).

In our work, we used alginate as a model of natural polysaccharides to study the heteroaggregation of CeO_2 NPs. An iron (III) oxide was chosen as an analogue of ICs as iron oxy-hydroxides was found to be one of the main inorganic components of the Lake Geneva water column (Graham et al., 2014). The aim of this study was to understand and establish the correlation between surface properties including surface charge, pH effect and concentration ratio with the importance of CeO_2 NP heteroaggregation in natural water. To fulfil this objective first, the heteroaggregation of a mixture composed of CeO_2 and Fe_2O_3 in absence and presence of 0.25 mg/L alginate and in increasing Fe_2O_3 concentration in ultrapure water was considered, and then filtered lake water was used. Second, the kinetics of heteroaggregation of individual components as well as mixtures of medium increasing complexity was studied. Finally, the effect of increasing alginate concentration on heteroaggregation was investigated.

2 Materials and Methods

2.1 Materials

Pristine CeO_2 NPs (powder NM-212, JRC, Ispra, Italy) with nominal particle diameter 28 ± 10 nm and a specific surface area equal to 27.2 ± 0.9 m^2g^{-1} (Singh et al., 2014) were used. To prepare a 1 gL^{-1} CeO_2 stock suspension, NP powder was weighed and diluted in ultrapure water (R > 18 MΩ cm, Millipore, Switzerland) at pH 3.0 to obtain a stable suspension. Then the dilution was done and in all further experiments a 50 mgL^{-1} CeO_2 suspension was used, unless indicated. The detailed characterisation of pristine NPs is provided in supplementary materials (SM) (Fig. 1 and Fig. SM.1). The stability of suspension was systematically controlled every time before performing the experiments by measuring z-average diameter and zeta potential.

Alginate (A2158, Sigma Aldrich, Switzerland) was used as a model of natural polysaccharide. A 100 mg/L stock solution was prepared in ultrapure water and used for further dilution. The detailed characterisation of alginate solution is shown in SM (Fig. SM.3).

As an analogue of inorganic colloids, iron (III) oxide (α-Fe_2O_3, 99%) (Nanoamor, Inc., USA) as a powder was used. A 1 g/L suspension was prepared and the suspension pH was set to 10. Such pH allowed a better resuspension and higher stability of dispersed particle. Probe sonication was done during 15 min. Then a 100 mg/L stock suspension was prepared by dilution with ultrapure water which pH was also previously adjusted to 10. The z-average hydrodynamic diameter and zeta-potential were measured as a function of pH in order to characterise obtained particle dispersion. Fe_2O_3 was found to have a negative surface charge at environmentally relevant pH (pH

153 8.0 ± 0.2). The detailed particle characterisation and titration curves are provided in Fig.
154 1 and in the SM (Fig. SM.2).

155 To mimic the ionic composition of Lake Geneva water, in particular the
156 concentration of divalent cations such as Ca^{2+} and Mg^{2+} two electrolytes were used. Two
157 stock solutions a 1 g/L of $CaCl_2 \cdot 6H_2O$ and $MgCl_2 \cdot 6H_2O$ (Fluka and Sigma-Aldrich,
158 Switzerland) were prepared. They were diluted and mixed to obtain a final solution that
159 represented synthetic water with ion concentrations equal to 45 mg/L for Ca^{2+} and 6
160 mg/L for Mg^{2+}.

161 Samples of natural water from Lake Geneva were collected in Versoix (Geneva,
162 Switzerland). The physicochemical characterisation was performed in situ using pH
163 (PHC101), conductivity (CDC401) and oxygen (LDO101) probes with multiparameter
164 meter (HQ40d) (Hach Lange, Switzerland). The water ionic composition was defined by
165 chromatographic analysis using a Dionex ICS-3000 analyzer (Dionex, Switzerland). The
166 detailed characterisation of lake water sample is provided in the SM (SM.1). Lake water
167 was filtered with a pore size equal to 0.45 µm before performing the experiments.

168 All stock solutions were stored in a dark place at 4 °C.

169

170 **2.2 Experimental procedures and methods**

171 Series of independent suspensions were prepared to investigate the effect of IC
172 concentration on the heteroaggregation of CeO_2 NPs. An aliquot of CeO_2 stock
173 suspension was added to ultrapure and lake water to obtain final concentration equal to
174 50 mg/L. Sodium hydroxide and hydrochloride acid 0.01 M (NaOH and HCl,
175 Titrisol®113, Merck, Switzerland) were used to adjust the pH to 8. Variable
176 concentrations of IC from 0 to 7.5 mg/L were added to ultrapure and lake waters before
177 the addition of CeO_2 suspension. The measurement of z-average hydrodynamic diameter

was done using a Malvern Zetasizer Nano ZS (*Malvern Instruments Ltd, UK*) directly (starting 30 sec after the mixture preparation) during 15 min with time interval 30 sec. The average value was calculated based on the last 3 min of experiments. Zeta potential was determined after the measurement of z-average diameter, i.e. 15 min after mixture was prepared. Alginate was added to ultrapure and lake water before the addition of NPs but after IC. The concentrations of the different compounds in kinetics experiments were equal to [CeO_2] = 50 mg/L [Fe_2O_3] = 5 mg/L, [Alginate] = 0.25 and 2 mg/L. The order of compounds addition was first water (ultrapure, synthetic, lake waters), then IC, if needed alginate and at the end CeO_2 NPs. The control of pH was done during all experiments with a Hach Lange HQ40d portable meter and pH probe PHC101 (Hach Lange, Switzerland).

All the experiments were performed at least in duplicates and the results given as mean values and standard deviations.

A JEOL JSM-7001FA scanning electron microscope (SEM) was used to obtain images of CeO_2 NPs in mixture with IC and in complex matrix. For each samples, 10 µL of the NPs dispersion were placed on one aluminum stub covered with a 5×5 mm silica wafer (Agar Scientific, G3390) and wrapped with 3 – 5 nm of Pt/Pd coating. The instrument was set with following parameters: voltage 15 kV, probe current 1 nA.

The aggregation kinetics experiments were investigated by time resolved dynamic light scattering (DLS) methods by measuring z-average diameters. Average value of z-average hydrodynamic diameter and standard deviation of this value were calculated by considered two neighbour points to plot the kinetics curves. The kinetic data of z-average hydrodynamic diameters, measured over the first 5 min after mixture preparation, were linearly fitted to obtain the slope and to calculate the aggregation rate (nm/min). Global attachment efficiency (α_{global}) was calculated also using time resolved

DLS method and represents the global behaviour of the system including homo- and heteroaggregation between pristine particles as well as NOM (Gallego-Urrea et al., 2016; Labille et al., 2015; Praetorius et al., 2014). The slope of the fitting line of the increase of z-average hydrodynamic diameters with time (first 5 min) for each particle mixture in different type of water is calculated. Attachment efficiencies were calculated by dividing these slopes for different water composition (i.e. in the reaction limited aggregation regime) by the slope of the diffusion limited aggregation regime determined under favourable conditions (i.e. critical coagulation concentration (CCC)) (Chen et al., 2006; Gallego-Urrea et al., 2016):

$$\alpha_{global} = \frac{k}{k_{\max}}, \qquad (1)$$

were k is the aggregation rate of the studied system at any specific moment (the reaction limited aggregation), k_{max} is the aggregation rate when all the collision between particles are efficient, i.e. results in the formation of permanent contacts (diffusion limited aggregation). Such type of aggregation usually occurred when the CCC is reached.

To determine the CCC, the homoaggregation of pristine CeO_2 NPs in increasing NaCl concentration was performed (SM, Fig. SM.8). Then the aggregation rates of different mixtures were divided by the aggregation rate at the CCC of CeO_2 NPs to obtain α_{global}. The graphical representation of attachment efficiency during homoaggregation (α_{homo}) in comparison to α_{global} is also presented in SM.

3. Results and discussion

Before performing the heteroaggregation experiments between CeO_2 NPs and inorganic colloids (Fe_2O_3 ICs) in natural waters, we studied the behaviour of uncoated pristine particles as well as coated with NOM in more simplified condition (such as ultrapure water). CeO_2 NPs, alginate and Fe_2O_3 ICs were also characterised by measuring the variation of zeta potentials and z-average hydrodynamic diameters with change of pH.

3.1 Characterisation of NPs and ICs

The zeta potential values as well as z-average diameters of both CeO_2 and Fe_2O_3 as a function of pH are presented in Fig. 1. CeO_2 NPs are positively charged below pH 6 whereas Fe_2O_3 ICs are positively charged below pH 5.0. Both are negatively charged above pH 7.0 and zeta potential is gradually decreasing with pH increase, from around +50 mV for CeO_2 and from +30 mV for Fe_2O_3 to around –45 mV and –35mV, accordingly. The pH_{PZC} was found equal to 6.8 ± 0.1 for CeO_2 and 5.8 ± 0.1 for Fe_2O_3, in accordance with other experimental data (Kosmulski, 2009; Yi et al., 2015). At environmental pH 8.0 ± 0.2 both NPs and ICs are negatively charged; zeta potential of CeO_2 is equal to –37.0 ± 0.4 and of Fe_2O_3 –27.1 ± 0.6. CeO_2 NPs are stable below pH 4 and above pH 8 with mean z-average diameter equal to 173.8 ± 7.8 nm. Fe_2O_3 ICs are stable in the same pH range but with slightly smaller diameter equal to 97.7 ± 2.5. Around the PZC both NPs and ICs are aggregated with diameter approaching 1800 nm for CeO_2 and 4500 nm for Fe_2O_3. Therefore, at the PZC the size of CeO_2 homoaggregates is smaller compared to the size of Fe_2O_3 homoaggregates. Such a behaviour is due to the different shapes of the pristine particles which result in the formation of more compact CeO_2 aggregates compared to Fe_2O_3. We performed SEM images of CeO_2 NPs and Fe_2O_3 ICs individually to gain insight into the morphology of homoaggregates and to be able to distinguish both types of particles in a mixture (SM.2, Fig. SM.1 and Fig. SM.2). We found that CeO_2 NPs have cubic

shape whereas Fe_2O_3 ICs exhibit long needle shaped particles. We also characterise alginate which is negatively charged across the full pH range with a z-average hydrodynamic diameter that not exceed 250 nm (Fig. SM.3).

3.2 CeO_2 NP heteroaggregation in presence of Fe_2O_3 ICs and alginate

Heteroaggregation of CeO_2 NPs in ultrapure water

To understand the heteroaggregation of CeO_2 NPs in presence of Fe_2O_3 ICs all experiments were performed at pH 8 to approach environmental conditions. We increased the concentration of Fe_2O_3 from 0 to 7.5 mg/L and measured zeta potentials (15 min after mixture preparation) and z-average hydrodynamic diameters (every 30 s during 15 min) in absence and presence of 0.25 mg/L alginate. At this pH both CeO_2 NPs and Fe_2O_3 ICs are negatively charged and no interaction was observed because of the electrostatic repulsions (Fig. 2). The average value of zeta potential was found equal to –37.1 ± 1.6 mV and z-average diameter to 177 ± 9 nm. Similar results, regarding heteroaggregation, were obtained by considering TiO_2 NPs and SiO_2 colloids (Praetorius et al., 2014). No heteroaggregation was observed at pH 8 (at low electrolyte concentration) because of the repulsive charges between particles. In presence of alginate, no significant change in the value of zeta potential (equal to –37.3 ± 1.5 mV) and z-average diameter (171 ± 8 nm) (Fig. 2 A and B) was observed due to the importance of repulsive interactions.

Heteroaggregation of CeO_2 NPs in lake water

We performed similar experiments as described in previous section but in filtered water from Lake Geneva to evaluate the importance of CeO_2 NP heteroaggregation in lake water. Interestingly, we observed a shift of particle zeta potential (for both cases in the presence and absence of alginate) to low values compared to ultrapure water. Zeta

potential became less negative and equal to –12.0 ± 0.4 mV without alginate and –14.8 ± 0.5 mV in the presence of alginate (Fig. 3A). The more negative value of zeta potential in the presence of alginate is due to the additional negative charges provided by alginate (Fig. SM.3). The difference of zeta potentials observed in ultrapure water compared to lake water was attributed to the presence of positively charged ions such as Na^+, K^+, Ca^{2+} and Mg^{2+} resulting in screening effects and specific adsorption on the negative NP surface. In such conditions, heteroaggregation of CeO_2 NPs was observed. Z-average diameter was found equal to 904 ± 148 nm without alginate and 370 ± 55 nm in the presence of 0.25 mg/L alginate (Fig. 3B). Alginate was found to reduce the aggregation rate process in lake water for pristine NPs due to stabilising effect (with alginate adsorption via cation bridging) (Oriekhova et al., 2017). The addition and increase of Fe_2O_3 concentration resulted in the increase of heteroaggregation with and without alginate. Below 1 mg/L Fe_2O_3 the aggregate z-average diameters were found less than 1000 nm (Fig. 3B). Increase of Fe_2O_3 concentration resulted in larger size of the aggregates, with z-average diameters close to 3000 nm. The presence of alginate was found to have no effect above 1 mg/L Fe_2O_3, therefore, indicating dominant effect of Fe_2O_3 concentration on heteroaggregation and z-average diameter measurements in such conditions.

3.3 Heteroaggregation kinetic experiments

The aim of this section was to investigate in details kinetics of heteroaggregation between CeO_2 NPs, Fe_2O_3 ICs and alginate. First, we studied the kinetics of homoaggregation of pristine CeO_2 and Fe_2O_3, then the heteroaggregation in mixtures of CeO_2 and alginate, and Fe_2O_3 and alginate. Finally, we studied the heteroaggregation of mixture CeO_2–Fe_2O_3 and of the system with including three compounds, i.e. CeO_2, Fe_2O_3

and alginate. We performed experiments first in ultrapure water and then in synthetic and in natural waters for a more detailed understanding of the interaction mechanisms.

Heteroaggregation kinetics in ultrapure water

As shown in Fig. 4, in which z-average hydrodynamic diameters of particles in ultrapure water at pH 8.0 are presented, CeO_2 NPs and Fe_2O_3 ICs are stable at pH 8. Mean value (15 min) of z-average diameters of pristine CeO_2 NPs is equal to 192 ± 6 nm and is stable during 15 min measurement. The presence of alginate slightly reduces the value of z-average diameters which is equal to 177 ± 9 nm. Z-average diameters of Fe_2O_3 ICs and Fe_2O_3 + alginate are equal to 147 ± 6 nm and 170 ± 10 nm, respectively. By considering a mixture of CeO_2 and Fe_2O_3 without alginate z-average diameter is equal to 181 ± 8 nm. This value is found between the diameters of CeO_2 and Fe_2O_3, indicating no interaction between NPs and ICs. The presence of alginate slightly reduces z-average diameter which is equal to 161 ± 8 nm. The most important point here is to note that no heteroaggregation is observed in the mixtures between CeO_2 and Fe_2O_3 and in the mixtures CeO_2/ Fe_2O_3/Alginate in ultrapure water due to the negative surface charges of all components as indicated by the zeta potential value presented in Table 1.

Heteroaggregation kinetics in lake water

The time variation of z-average hydrodynamic diameters of CeO_2 NPs, Fe_2O_3 ICs, and mixtures of NPs and ICs in the presence and absence of alginate in filtered Lake Geneva water is presented in Fig. 5A. Pristine CeO_2 NPs are forming aggregates in lake water (black squares) with z-average dimeter equals to 1065 ± 19 nm after 15 min. Aggregation is promoted due to the presence of divalent electrolytes, dissolved organic matter and natural colloids (Louie et al., 2013; Oriekhova and Stoll, 2016). The presence of alginate reduces the aggregation rate of CeO_2 NPs from 50 ± 8 nm/min to 19 ± 4 nm/min (Fig. 5B). The value of the z-average diameter is also decreased and is found

equal to 434 ± 10 nm. Moreover, zeta potential of CeO_2 NPs in the presence of alginate decreases compared to pristine particle and is equal to -15.0 ± 0.6 versus -12.3 ± 0.5 mV (Table 1) indicating NP surface coating by alginate and alginate stabilisation effect.

Table 1. Zeta potentials in different water samples (pH 8.0 ± 0.2)

Pristine Fe_2O_3 ICs are also aggregated in lake water (red circles) with z-average diameter equals to 2236 ± 90 nm. The aggregation rate of Fe_2O_3 ICs is higher compared to the aggregation rate of CeO_2 NPs indicating that Fe_2O_3 aggregates growth faster compared to CeO_2 NPs. We believe it is due to the Fe_2O_3 shape resulting in formation of more extended structures and less compact aggregates. In the presence of alginate, Fe_2O_3 ICs are found to have larger aggregate sizes (3051 ± 172 nm) due to the bridging effect in presence of alginate. Heteroaggregation between CeO_2 NPs and Fe_2O_3 ICs in lake water is occurring now since it was not the case in ultrapure water (Fig. 4). Heteroaggregation is due to the presence of natural ions (Ca^{2+}, Mg^{2+}) and organic substances which specifically adsorb on the surface of both NPs and ICs changing their surface chemistry. The presence of alginate does not have an effect on heteroaggregation in a mixture CeO_2 + Fe_2O_3 (Fig. 5A). In a mixture of NPs and ICs and in natural water alginate does not have an effect on the size of heteroaggregates. In addition, the size of Fe_2O_3 aggregates is similar to the size of mixtures, probably, because of the main role of Fe_2O_3 in the process of aggregate formation.

Heteroaggregation kinetics in synthetic water

It is known that divalent cations have a significant effect on the NP stability (Chekli et al., 2015; Liu et al., 2013; Loosli et al., 2015). Regarding the results obtained in previous section and in order to specifically evaluate the effect of divalent cations, synthetic water

containing the same amount of Ca^{2+} and Mg^{2+} as in Lake Geneva water was prepared (more details in section 2.1). The time variation of z-average hydrodynamic diameters presented in Fig. 6A indicates that the same trend as in lake water is observed. Pristine CeO_2 and Fe_2O_3 are aggregated in synthetic water and the aggregation rate is slightly increased for CeO_2 and stays similar for Fe_2O_3 (62 ± 6 and 95 ± 13 nm/min, accordingly) compared to the aggregation rate in lake water 50 ± 8 and 89 ± 18 nm/min, accordingly. Aggregation is due to both charge screening and specific adsorption of cations which lead to the destabilisation of NPs and mixtures. The presence of alginate also slightly reduces the aggregation rate for NPs but has no effect on Fe_2O_3 and on the CeO_2 + Fe_2O_3 mixture (Fig. 6B). However, the effect of naturally present organic matter is clearly reflected on zeta potential values (Table 1). Very interestingly, in synthetic water the presence of divalent electrolytes only results in lower value of zeta potential, whereas in lake water zeta potentials are more negative because of the presence of natural organic matter. Therefore, this comparative study between synthetic and natural waters highlighted the key role of divalent electrolytes in the heteroaggregation of NPs in lake water.

3.4 Effect of alginate concentration on heteroaggregation in lake water

To gain an insight into the effect of alginate concentration we studied the heteroaggregation between CeO_2 NPs and Fe_2O_3 in lake water by increasing the concentration of alginate from 0.25 to 2 mg/L (Fig. 7). Without alginate and in the presence of 0.25 mg/L alginate, z-average diameters are found close to 2500 nm (after 15 min heteroaggregation). The presence of 2 mg/L alginate is found to significantly reduce the size of the aggregates equal to 608 ± 45 nm (after 15 min) (Fig. 7). The aggregation rate is also significantly reduced and is found equal to 125 ± 41 and 15 ± 2

nm/min (Fig. SM.6) in the presence of 0.25 and 2 mg/L alginate, accordingly, in good agreement with stabilisation effects related to electrostatic and steric effects (Baalousha, 2009; Oriekhova and Stoll, 2016). Our findings are also supported with SEM images (Fig. 8). In Fig. 8A and B large heteroaggregates of CeO_2 and Fe_2O_3 are found and no significant difference is observed at low alginate concentrations. Whereas in Fig. 8C heteroaggregates are much smaller and it is possible to distinguish the presence of Fe_2O_3 connected by alginate and "individual" alginate chains on the surface of silica wafer. Therefore, in our work we showed that high alginate concentration prevent the heteroaggregation of mixtures of CeO_2 NPs and Fe_2O_3 ICs in lake water. It should be noted that the same trend was observed in synthetic water (Fig. SM.7) where the increase of alginate concentration was found to decrease the aggregation rate but less significantly compared to lake water.

The global attachment efficiency (α_{global}) which is a mixture of the attachment efficiencies of homo- and heteroaggregation (Labille et al., 2015) is given in Fig. 9. This figure is presenting the attachment efficiencies calculated from experimental data of pristine CeO_2 NPs and Fe_2O_3 ICs as well as their mixtures in synthetic and lake waters as a function of alginate concentration. The presence of alginate decreases the global attachment efficiency of heteroaggregates. We also observe that the attachment efficiency between pristine CeO_2 NPs is lower than between Fe_2O_3 ICs. We also shown that in mixture without alginate and at low alginate concentration the attachment efficiency is larger than 1 indicating faster formation of heteroaggregates compared to pristine CeO_2 NPs at high ionic strength (CCC), i.e. during the diffusion limited aggregation (Metreveli et al., 2015).

4. Conclusions

Our findings demonstrate that heteroaggregation between CeO_2 NPs and Fe_2O_3 ICs is highly dependent on the resulting electrostatic scenarios and presence of divalent ions in the solution. In ultrapure water, no heteroaggregation between NPs and ICs is observed because of the electrostatic repulsions due to the presence of negative charges. On the other hand, in natural lake and synthetic waters, in presence of divalent ions (such as Ca^{2+} and Mg^{2+}), CeO_2 heteroaggregation is observed due to the formation of bridges between the different negatively charged compounds. The concentration of alginate plays also a crucial role in controlling heteroaggregation in natural waters. In absence and at low alginate concentration (below 0.25 mg/L) significant heteroaggregation is observed, whereas, high alginate concentration (2 mg/L and above) prevents heteroaggregation. Our results indicate that both water hardness and natural organic matter concentration are key parameters to consider when evaluating the importance of heteroaggregation, determination of attachment efficiencies, and prediction of NPs in transport models including both homo and heteroaggregation processes.

Acknowledgements.

The authors acknowledge support receive from the European Commission and the Swiss Secrétariat d'Etat à la Formation et à la Recherche et à l'Innovation SEFRI within the Horizon 2020 Program (NanoFASE 15.0183-2, 646002) and University of Geneva. Authors are also grateful to Agathe Martignier for her support during the SEM measurements.

422

423 **Table 1.** Zeta potentials in different water samples (pH 8.0 ± 0.2)

Name of the sample	Ultrapure	Lake Geneva	Synthetic water
CeO_2	-40.3 ± 2.6	-12.3 ± 0.5	-2.0 ± 0.2
Fe_2O_3	-24.9 ± 1.6	-10.6 ± 0.4	-3.9 ± 0.3
CeO_2 + Fe_2O_3	-34.3 ± 1.4	-10.8 ± 0.4	-2.7 ± 0.3
CeO_2 + Alginate	-39.2 ± 1.4	-15.0 ± 0.6	-14.8 ± 0.4
Fe_2O_3 + Alginate	-27.5 ± 0.7	-14.4 ± 0.4	-13.4 ± 0.4
CeO_2 + Fe_2O_3 + Alginate	-36.9 ± 2.1	-13.8 ± 0.5	-9.9 ± 0.4

424

425

Figures

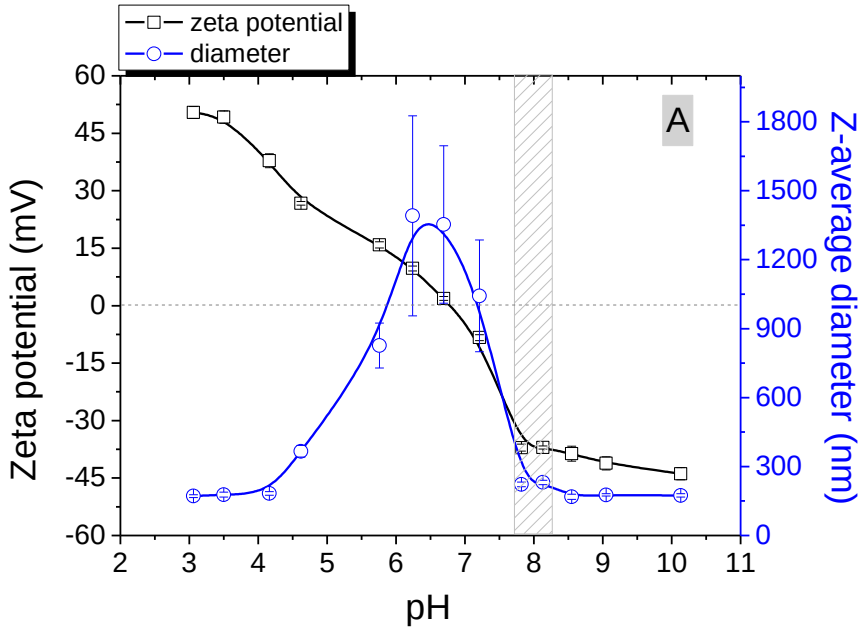

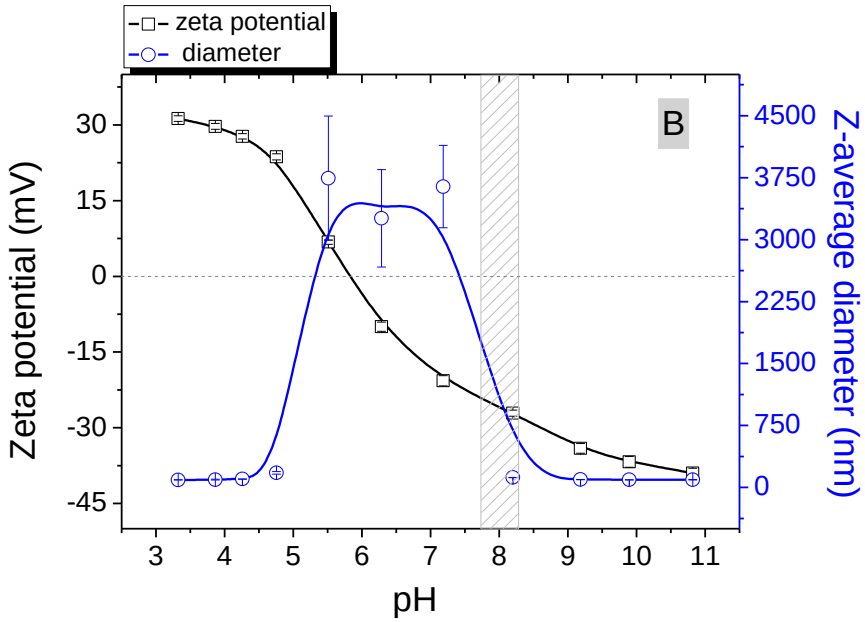

Fig.1. (A) CeO_2 NP and (B) Fe_2O_3 IC zeta potential and z-average hydrodynamic diameter variation as a function of pH. Experimental conditions: [CeO_2] = 50 mg/L, [Fe_2O_3] = 10 mg/L. No electrolytes were added to the NP suspensions. At environmental pH = 8.0 ± 0.2 both NPs and ICs are negatively charged. Each point represents the mean value of five parallel experiments and error bars represent the standard deviation.

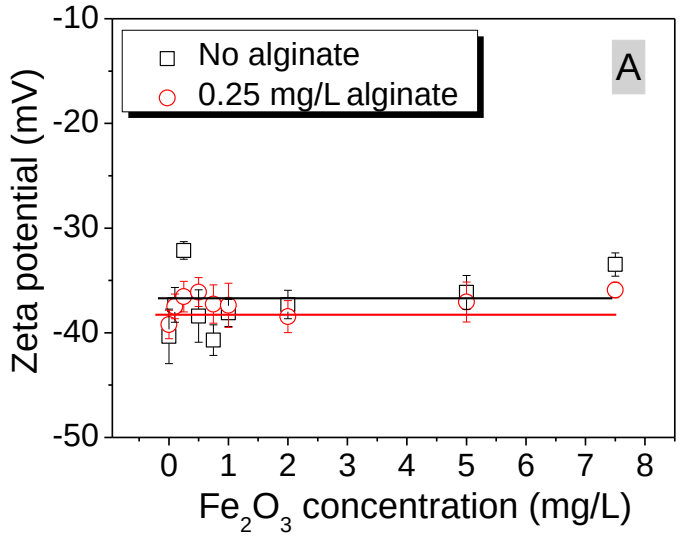

435

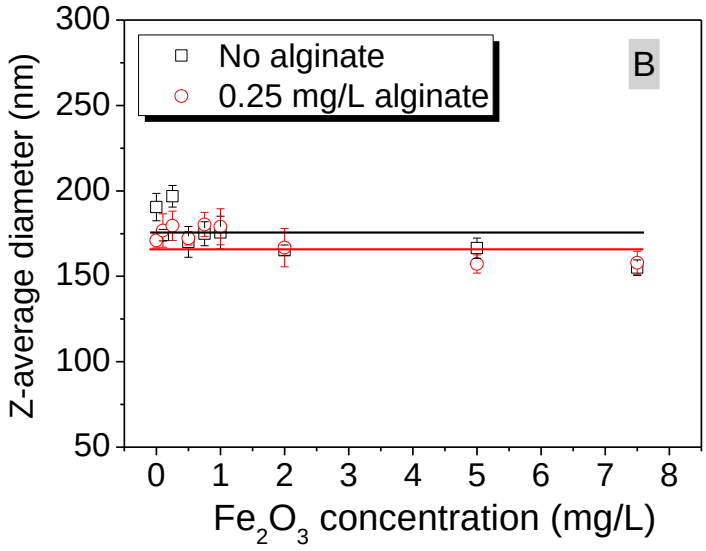

436

437 **Fig. 2.** (A) Zeta potential and (B) z-average hydrodynamic diameters of CeO_2 NPs in
438 ultrapure water at different concentrations of inorganic colloids (Fe_2O_3) in presence and
439 absence of alginate. Experimental conditions: pH 8.0 ± 0.2, [CeO_2] = 50 mg/L, [Alginate]
440 = 0.25 mg/L. No heteroaggregation between NPs, ICs and alginate is observed. Error
441 bars of zeta potential represent standard deviations of duplicates. Each z-average
442 diameter value represents the average value of last 3 min measurements and error bars
443 represent standard deviations.

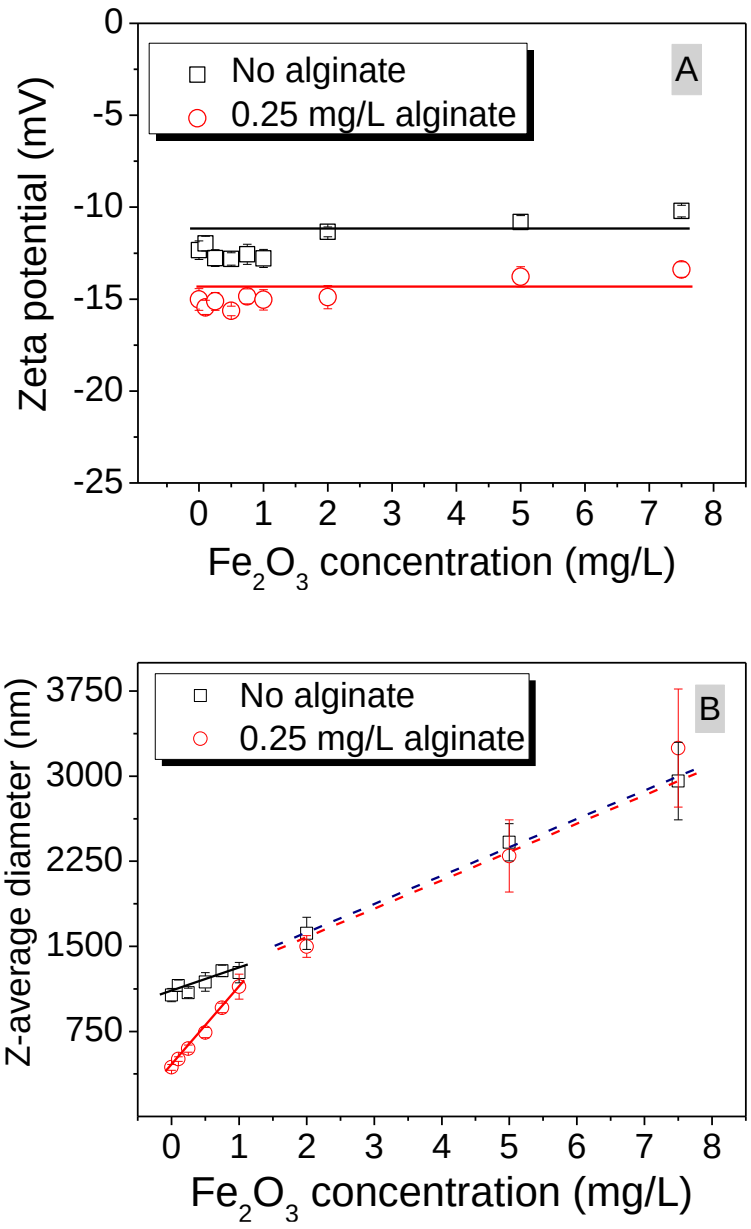

Fig. 3. (A) Zeta potential and (B) z-average hydrodynamic diameters of CeO_2 NPs in lake water in increasing concentration of inorganic colloids (Fe_2O_3) in presence and absence of alginate. Experimental conditions: pH 8.0 ± 0.2, [CeO_2] = 50 mg/L, [Alginate] = 0.25 mg/L. Heteroaggregation is observed with increase of IC concentration both in absence and presence of alginate. Error bars of zeta potential represent standard deviations of duplicates. Each z-average diameter value represents the average value of last 3 min measurements and error bars represent standard deviations.

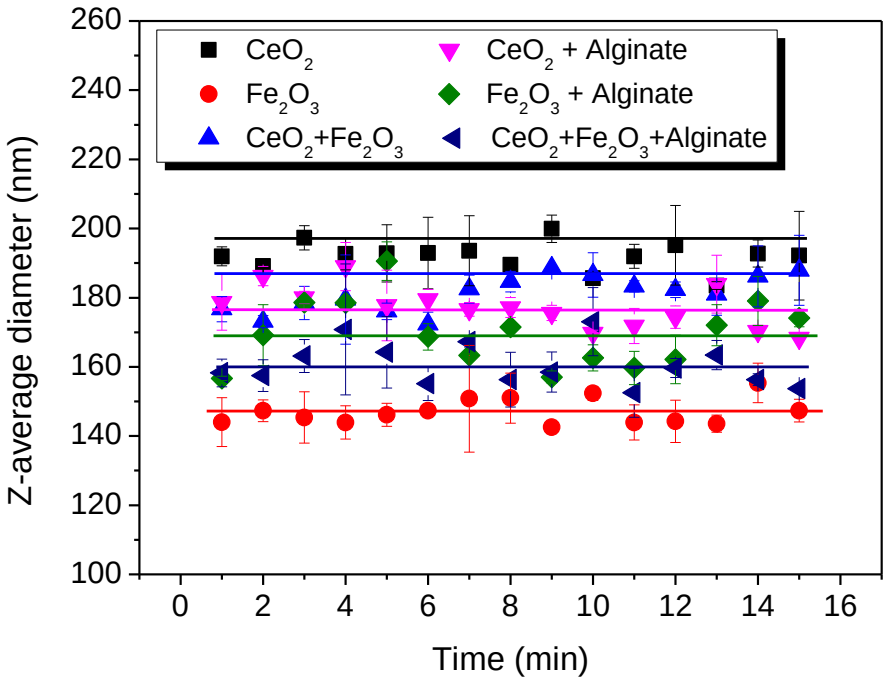

Fig. 4. Z-average hydrodynamic diameters of CeO_2 NPs in varied conditions: in the presence of inorganic colloids and alginate at pH > pH_{PZC} in ultrapure water. No interactions between CeO_2 NPs, Fe_2O_3 IC and alginate is observed. Experimental conditions: pH 8.0 ± 0.2, [CeO_2] = 50 mg/L [Fe_2O_3] = 5 mg/L, [Alginate] = 0.25 mg/L. Error bars represent standard deviations of duplicates. Horizontal lines are used to guide the eyes and are drawn in the error limits.

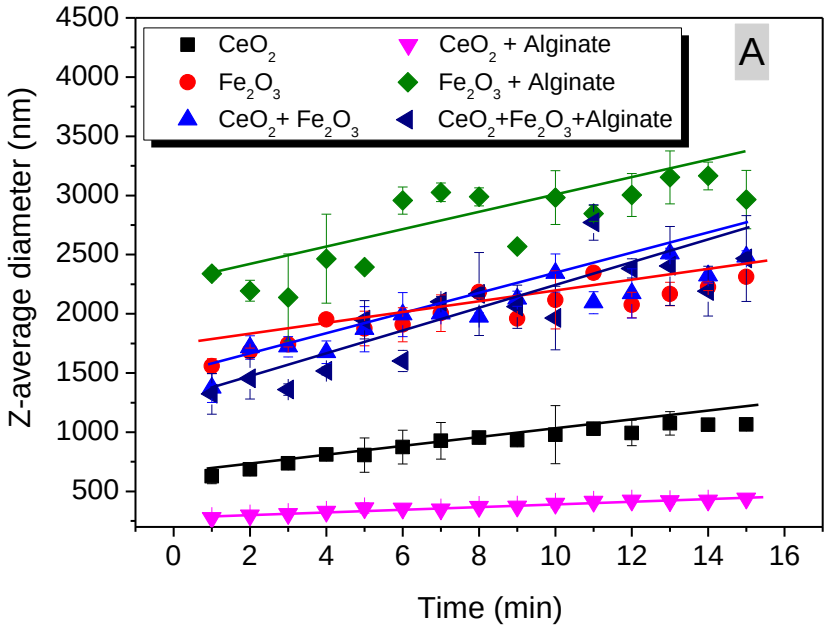

464

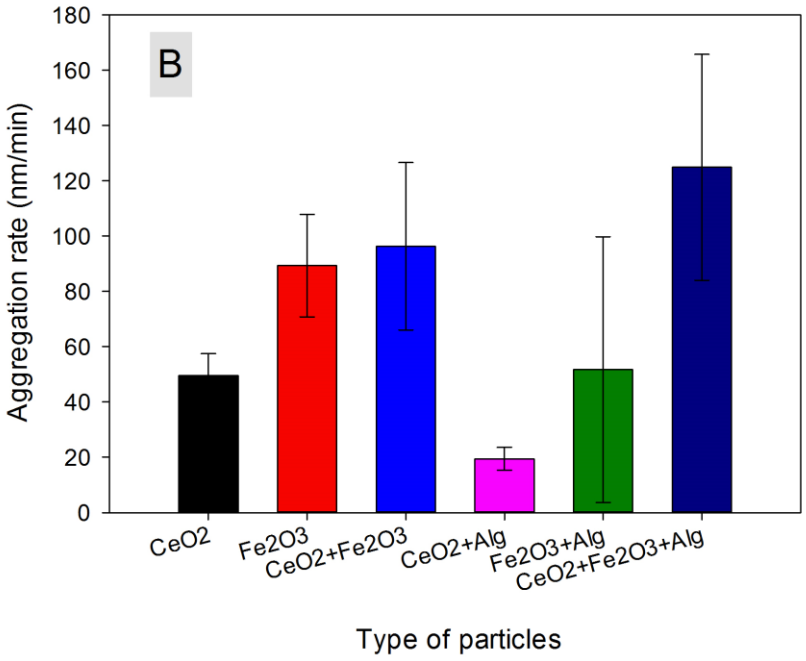

465

466

467 **Fig. 5.** (A) Z-average hydrodynamic diameters and (B) aggregation rate of CeO_2 NPs in
468 Lake Geneva water: in the presence of Fe_2O_3 ICs and alginate. Experimental conditions:
469 pH 8.0 ± 0.2, [CeO_2] = 50 mg/L [Fe_2O_3] = 5 mg/L, [Alginate] = 0.25 mg/L. Error bars
470 represent standard deviations of duplicates.

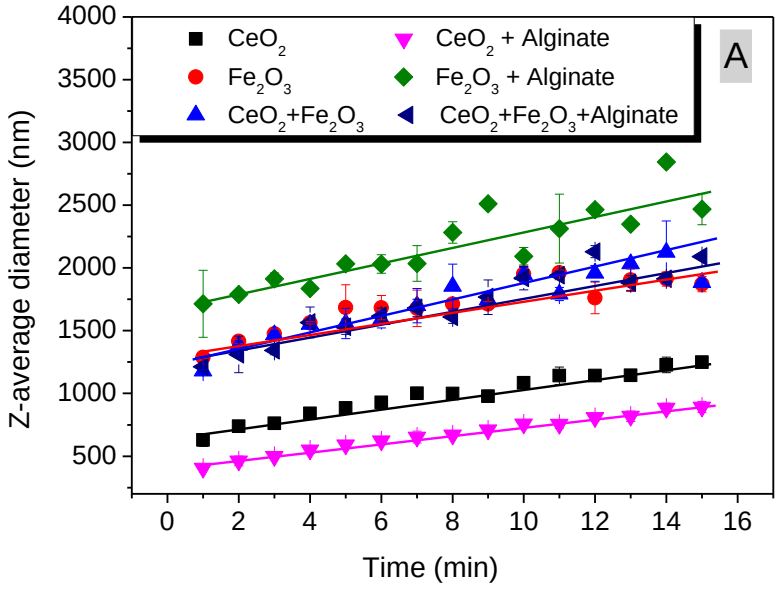

471

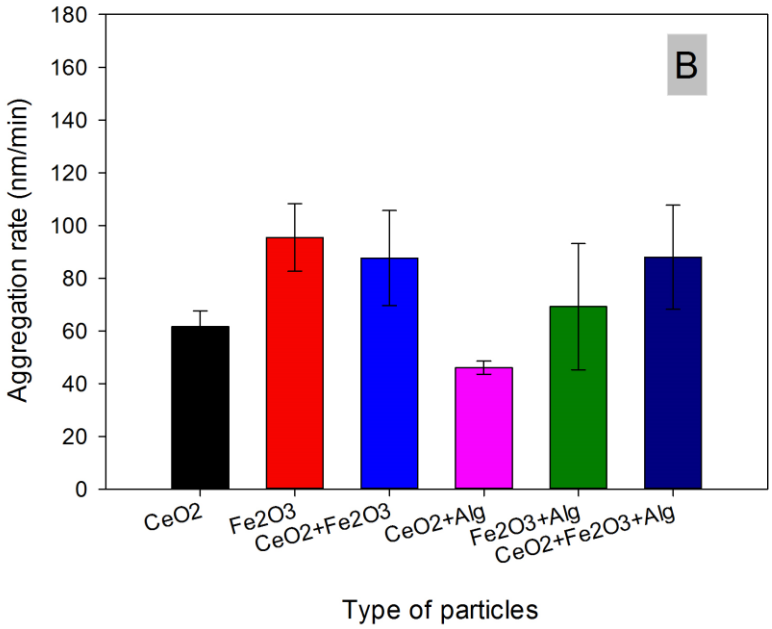

472

473

474 **Fig. 6.** (A) Z-average hydrodynamic diameters and (B) aggregation rate of CeO_2 NPs in
475 synthetic water (in the presence of Ca^{2+}/Mg^{2+} ions) and in the simultaneous presence of
476 Fe_2O_3 ICs and alginate. Experimental conditions: pH 8.0 ± 0.2, [CeO_2] = 50 mg/L [Fe_2O_3]
477 = 5 mg/L, [Alginate] = 0.25 mg/L. Error bars represent standard deviations of
478 duplicates.

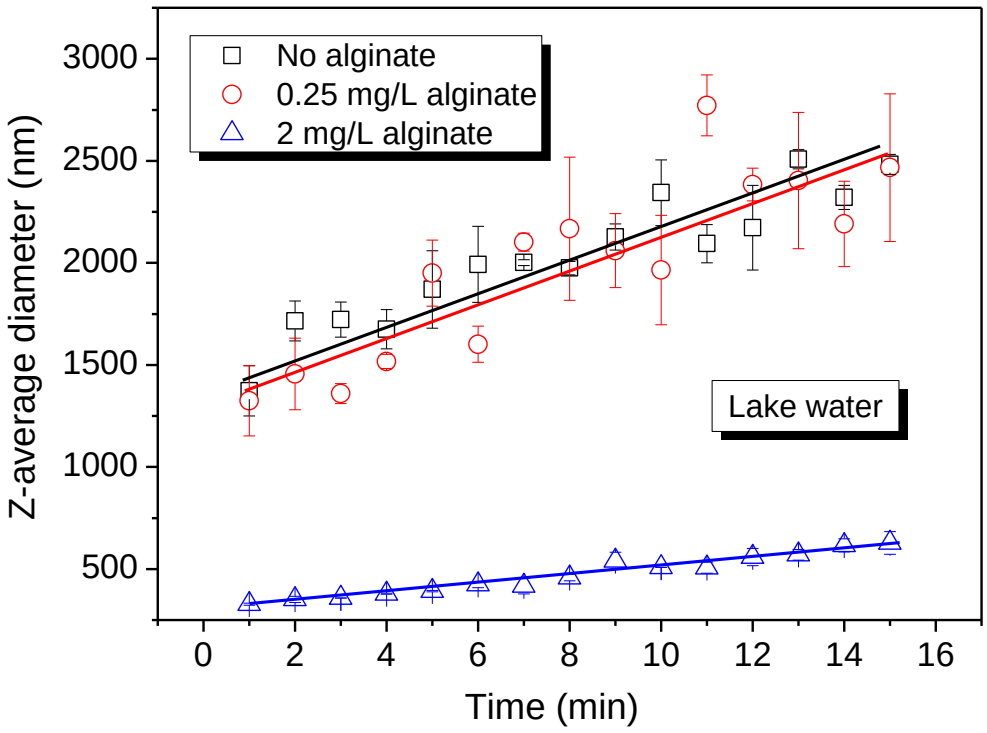

479

480 **Fig. 7.** Time variation of z-average hydrodynamic diameters of CeO_2 NPs and Fe_2O_3 ICs
481 in Lake Geneva in varied alginate concentration. Experimental conditions: pH 8.0 ± 0.2,
482 [CeO_2] = 50 mg/L [Fe_2O_3] = 5 mg/L, [Alginate] = 0.25 and 2 mg/L. The aggregation rate
483 decreases with increase of alginate concentration. Error bars represent standard
484 deviations of duplicates.

485

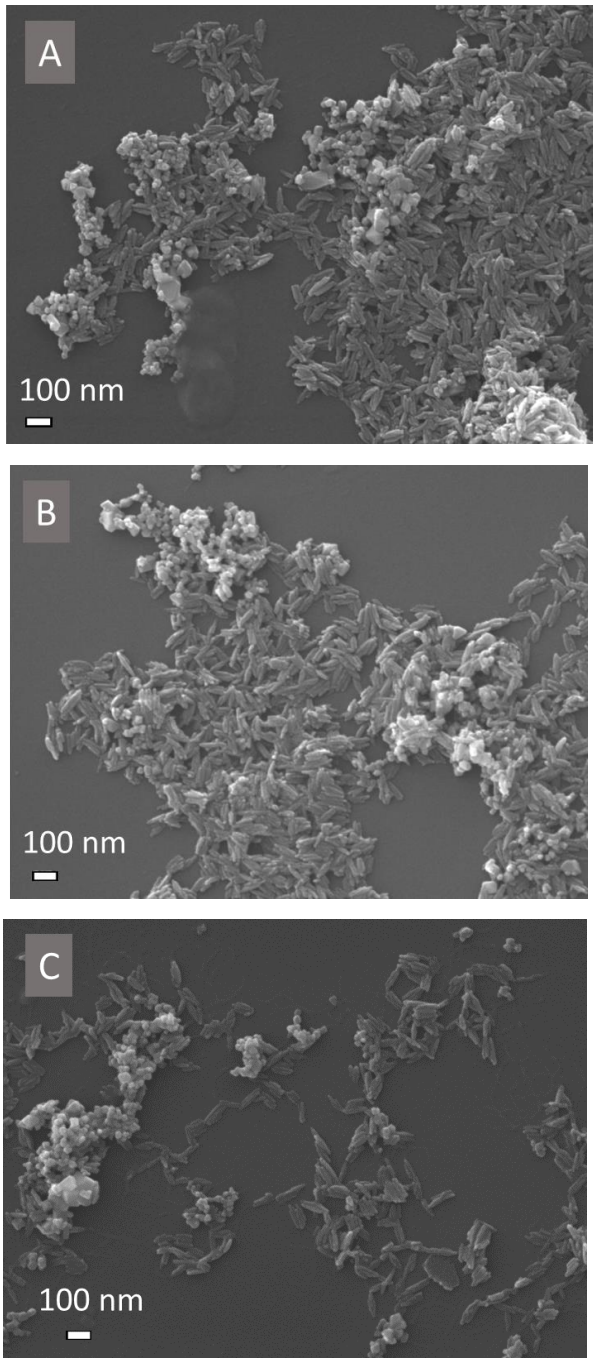

Fig. 8. SEM images of CeO_2 NPs and Fe_2O_3 ICs in Lake Geneva in varied alginate concentration. Experimental conditions: [CeO_2] = 10 mg/L [Fe_2O_3] = 1 mg/L (A): [Alginate] = 0 mg/L; (B) [Alginate] = 0.05 mg/L and (C) [Alginate] = 2 mg/L. With increase of alginate concentration, we observed the formation of smaller heteroaggregates corresponding to the results illustrated in Fig. 6.

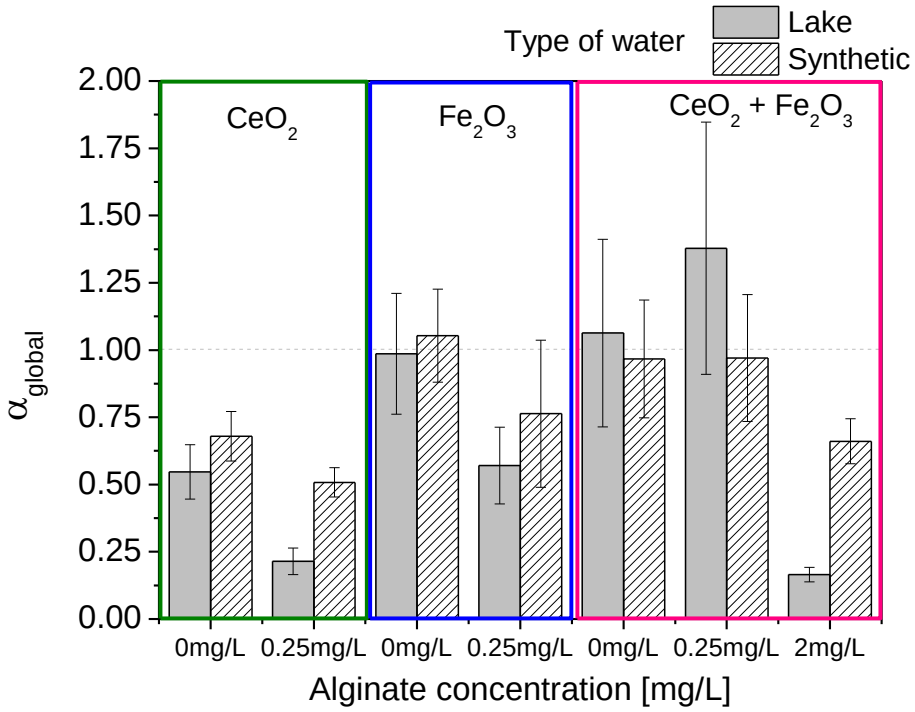

496

497 **Fig. 9.** The global attachment efficiency (α_{global}) of pristine CeO_2 NPs (green rectangle),
498 pristine Fe_2O_3) IC (blue rectangle) and of a mixture NPs + ICs in synthetic and lake
499 waters as a function of alginate concentration. Experimental conditions: pH 8.2 ± 0.2,
500 [CeO_2] = 50 mg/L, [Fe_2O_3] = 5 mg/L, [Alginate] = 0; 0.25 and 2 mg/L. Error bars
501 represent relative standard deviations of division (calculated for the ratio k/k_{max}).

502

503

References

Baalousha, M., 2009. Aggregation and disaggregation of iron oxide nanoparticles: Influence of particle concentration, pH and natural organic matter. Sci. Total Environ. 407, 2093–2101. https://doi.org/10.1016/j.scitotenv.2008.11.022

Buffle, J., Wilkinson, K.J., Stoll, S., Filella, M., Zhang, J., 1998. A Generalized Description of Aquatic Colloidal Interactions: The Three-colloidal Component Approach. Environ. Sci. Technol. 32, 2887–2899. https://doi.org/10.1021/es980217h

Castelló, J., Gallardo, M., Busquets, M.A., Estelrich, J., 2015. Chitosan (or alginate)-coated iron oxide nanoparticles: A comparative study. Colloids Surf. Physicochem. Eng. Asp. 468, 151–158. https://doi.org/10.1016/j.colsurfa.2014.12.031

Chekli, L., Zhao, Y.X., Tijing, L.D., Phuntsho, S., Donner, E., Lombi, E., Gao, B.Y., Shon, H.K., 2015. Aggregation behaviour of engineered nanoparticles in natural waters: Characterising aggregate structure using on-line laser light scattering. J. Hazard. Mater. 284, 190–200. https://doi.org/10.1016/j.jhazmat.2014.11.003

Chen, K.L., Mylon, S.E., Elimelech, M., 2006. Aggregation kinetics of alginate-coated hematite nanoparticles in monovalent and divalent electrolytes. Environ. Sci. Technol. 40, 1516–1523.

Eyrolle, F., Charmasson, S., 2004. Importance of colloids in the transport within the dissolved phase (< 450 nm) of artificial radionuclides from the Rhône river towards the Gulf of Lions (Mediterranean Sea). J. Environ. Radioact. 72, 273–286.

Eyrolle, F., Charmasson, S., 2001. Distribution of organic carbon, selected stable elements and artificial radionuclides among dissolved, colloidal and particulate phases in the Rhône River (France): Preliminary results. J. Environ. Radioact. 55, 145–155. https://doi.org/10.1016/S0265-931X(00)00188-0

Filella, M., 2007. Colloidal properties of submicron particles in natural waters. IUPAC Ser. Anal. Phys. Chem. Environ. Syst. 10, 17.

Gallego-Urrea, J.A., Hammes, J., Cornelis, G., Hassellöv, M., 2016. Coagulation and sedimentation of gold nanoparticles and illite in model natural waters: Influence of initial particle concentration. NanoImpact 3–4, 67–74. https://doi.org/10.1016/j.impact.2016.10.004

Gondikas, A.P., Kammer, F. von der, Reed, R.B., Wagner, S., Ranville, J.F., Hofmann, T., 2014. Release of TiO2 nanoparticles from sunscreens into surface waters: a one-year survey at the old Danube recreational Lake. Environ. Sci. Technol. 48, 5415–5422.

Graham, N.D., Stoll, S., Loizeau, J.-L., 2014. Colloid characterization at the sediment-water interface of Vidy Bay, Lake Geneva. Fundam. Appl. Limnol. Für Hydrobiol. 184, 87–100.

Kosmulski, M., 2009. Compilation of PZC and IEP of sparingly soluble metal oxides and hydroxides from literature. Adv. Colloid Interface Sci. 152, 14–25. https://doi.org/10.1016/j.cis.2009.08.003

Labille, J., Harns, C., Bottero, J.-Y., Brant, J., 2015. Heteroaggregation of Titanium Dioxide Nanoparticles with Natural Clay Colloids. Environ. Sci. Technol. 49, 6608–6616. https://doi.org/10.1021/acs.est.5b00357

Liu, J., Legros, S., Von der Kammer, F., Hofmann, T., 2013. Natural organic matter concentration and hydrochemistry influence aggregation kinetics of functionalized engineered nanoparticles. Environ. Sci. Technol. 47, 4113–4120.

551 Loosli, F., Coustumer, P.L., Stoll, S., 2013. TiO2 nanoparticles aggregation and
552 disaggregation in presence of alginate and Suwannee River humic acids. pH and
553 concentration effects on nanoparticle stability. Water Res. 47, 6052–6063.
554 Loosli, F., Le Coustumer, P., Stoll, S., 2015. Effect of electrolyte valency, alginate
555 concentration and pH on engineered TiO2 nanoparticle stability in aqueous
556 solution. Sci. Total Environ., Special Issue: Engineered nanoparticles in soils and
557 waters 535, 28–34. https://doi.org/10.1016/j.scitotenv.2015.02.037
558 Louie, S.M., Tilton, R.D., Lowry, G.V., 2013. Effects of Molecular Weight Distribution and
559 Chemical Properties of Natural Organic Matter on Gold Nanoparticle Aggregation.
560 Environ. Sci. Technol. 47, 4245–4254. https://doi.org/10.1021/es400137x
561 Metreveli, G., Philippe, A., Schaumann, G.E., 2015. Disaggregation of silver nanoparticle
562 homoaggregates in a river water matrix. Sci. Total Environ., Special Issue:
563 Engineered nanoparticles in soils and waters 535, 35–44.
564 https://doi.org/10.1016/j.scitotenv.2014.11.058
565 Oriekhova, O., Le Coustumer, P., Stoll, S., 2017. Impact of biopolymer coating on the
566 colloidal stability of manufactured CeO2 nanoparticles in contrasting water
567 conditions. Colloids Surf. Physicochem. Eng. Asp. 533, 267–274.
568 https://doi.org/10.1016/j.colsurfa.2017.07.069
569 Oriekhova, O., Stoll, S., 2016. Stability of uncoated and fulvic acids coated manufactured
570 CeO2 nanoparticles in various conditions: From ultrapure to natural Lake Geneva
571 waters. Sci. Total Environ. 562, 327–334.
572 https://doi.org/10.1016/j.scitotenv.2016.03.184
573 Pawar, S.N., Edgar, K.J., 2012. Alginate derivatization: A review of chemistry, properties
574 and applications. Biomaterials 33, 3279–3305.
575 https://doi.org/10.1016/j.biomaterials.2012.01.007
576 Piccinno, F., Gottschalk, F., Seeger, S., Nowack, B., 2012. Industrial production quantities
577 and uses of ten engineered nanomaterials in Europe and the world. J.
578 Nanoparticle Res. 14, 1–11. https://doi.org/10.1007/s11051-012-1109-9
579 Praetorius, A., Labille, J., Scheringer, M., Thill, A., Hungerbühler, K., Bottero, J.-Y., 2014.
580 Heteroaggregation of Titanium Dioxide Nanoparticles with Model Natural
581 Colloids under Environmentally Relevant Conditions. Environ. Sci. Technol. 48,
582 10690–10698. https://doi.org/10.1021/es501655v
583 Quik, J.T.K., Stuart, M.C., Wouterse, M., Peijnenburg, W., Hendriks, A.J., van de Meent, D.,
584 2012. Natural colloids are the dominant factor in the sedimentation of
585 nanoparticles. Environ. Toxicol. Chem. 31, 1019–1022.
586 https://doi.org/10.1002/etc.1783
587 Singh, C., Friedrichs, S., Ceccone, G., Gibson, N., Jensen, K.A., Levin, M., Infante, H.G.,
588 Carlander, D., Rasmussen, K., 2014. Cerium Dioxide, NM-211, NM-212, NM-213.
589 Characterisation and test item preparation. European Commission, Joint
590 Research Centre, European Union. https://doi.org/10.2788/80203
591 Slomberg, D.L., Ollivier, P., Radakovitch, O., Baran, N., Sani-Kast, N., Miche, H.,
592 Borschneck, D., Grauby, O., Bruchet, A., Scheringer, M., Labille, J., 2016.
593 Characterisation of suspended particulate matter in the Rhone River: insights
594 into analogue selection. Environ. Chem.
595 Wang, H., Adeleye, A.S., Huang, Y., Li, F., Keller, A.A., 2015. Heteroaggregation of
596 nanoparticles with biocolloids and geocolloids. Adv. Colloid Interface Sci., Colloid
597 and Polymer Interfaces in Bio-resources and Environments 226, Part A, 24–36.
598 https://doi.org/10.1016/j.cis.2015.07.002

599 Yi, P., Pignatello, J.J., Uchimiya, M., White, J.C., 2015. Heteroaggregation of cerium oxide
600 nanoparticles and nanoparticles of pyrolyzed biomass. Environ. Sci. Technol. 49,
601 13294–13303.
602